

Alginate/guacamole edible films as moisture barrier layers in multicomponent foods

Matheus Carvalho de Matos^{1,2} | Jackson Andson de Medeiros^{1,3} |
Leticia Bueno Santos^{1,3} | Henriette M. C. de Azeredo¹ 

¹Embrapa Instrumentation, São Carlos, São Paulo, Brazil

²Graduate Program in Biotechnology, Federal University of São Carlos (UFSCar), São Carlos, São Paulo, Brazil

³Graduate Program in Food, Nutrition, and Food Engineering, Campus Araraquara, São Paulo State University (UNESP), Araraquara, São Paulo, Brazil

Correspondence

Henriette M. C. de Azeredo, Embrapa Instrumentation, R. 15 de Novembro, 1452, Caixa Postal 741, São Carlos, SP 13560-970, Brazil.
Email: henriette.azedero@embrapa.br

Funding information

Coordenação de Aperfeiçoamento de Pessoal de Nível Superior, Grant/Award Number: 88887.706251/2022-00; Conselho Nacional de Desenvolvimento Científico e Tecnológico, Grant/Award Numbers: 134100/2019-0, 161930/2021-2, 308777/2021-2

Abstract

In multicomponent foods having both moist and dry components (e.g., pizzas and tacos), moisture migration between components causes undesirable texture changes (e.g., loss of crispiness of the dry component). In this study, different proportions of alginate (film matrix), guacamole (hydrophobic component with sensory appeal), and glycerol (plasticizer) were combined to form edible films to be used as a moisture barrier between moist and dry components of multicomponent foods. Alginate was the component that most contributed to increase the film strength and to reduce its water vapor permeability (WVP). Guacamole, due to the presence of avocado lipids, enhanced the film hydrophobicity, although not having decreased the WVP (as expected), since it promoted discontinuities in the alginate structure. The film with the lowest WVP (containing an alginate/guacamole/glycerol dry mass ratio of 25/60/15) was inserted between nachos and tomato sauce, being able to reduce the crispiness loss of nachos during a 50-min storage.

KEYWORDS

biopolymers, mixture design, polysaccharides, water activity

1 | INTRODUCTION

Edible films are thin layers typically formed from casting and drying an (usually) aqueous dispersion containing a film-forming macromolecule, generally added with a plasticizing agent and/or other components, depending on the intended application. Edible films containing fruit purees or fruit juices have been proposed in several studies (Azeredo et al., 2016; Melo et al., 2019; Munhoz et al., 2018; Viana et al., 2018), the fruit purees not only providing the films with the sensory and functional properties of the fruits, but also plasticizing effects by sugars and organic acids. Films containing fruit purees are interesting for applications in which their sensory properties are appealing, such as sushi wraps, pouches that melt on cooking, or even snacks (Azeredo et al., 2022; Otoni et al., 2017).

Another interesting application for fruit-containing edible films is as a barrier layer between a dry and crispy component and a humid one in multilayer foods such as pizzas, wraps, and tacos (Azeredo et al., 2022). In times when food delivery services are booming, especially after the emergence of the COVID-19 pandemics (Oliveira et al., 2021), this kind of application is especially important, since the time between food preparation and consumption is longer than usual, which results in texture changes, particularly loss of crispiness, which has been a challenge for manufacturers, ingredient suppliers, restaurants, and packaging designers (Kelso, 2019).

Matrices of edible films are usually based on polysaccharides, whose hydrophilicity makes them poor barriers to water. Sodium alginate, which is a copolymer composed of 1,4- β -D-manuronic acid (M) blocks interspersed with

This is an open access article under the terms of the Creative Commons Attribution License, which permits use, distribution and reproduction in any medium, provided the original work is properly cited.

© 2023 The Authors. *eFood* published by John Wiley & Sons Australia, Ltd on behalf of International Association of Dietetic Nutrition and Safety.

1,4- α -L-guluronic acid (G) blocks, isolated from brown algae, has been used as a matrix for several edible films and wraps with good tensile and barrier properties, some of them containing fruit or vegetable purees, such as kale puree-based wraps (Oliveira et al., 2023), apple puree- (Kadzińska et al., 2020), and papaya puree-based edible films (Rangel-Marrón et al., 2019).

The presence of lipid-rich components may provide those films with lower water permeability, making them more suitable for applications that require inhibited moisture migration between components of multilayer foods. As an example, hydroxypropyl methyl cellulose (HPMC)-beeswax films were shown to significantly reduce the moisture migration in a model cheese-bread system (O'Connor et al., 2018).

The objective of this study is to develop an edible alginate-based film containing guacamole (as a component with sensory appeal and the hydrophobic properties of avocado lipids) to be applied as a barrier layer to reduce moisture migration between food layers with different water activities.

2 | MATERIALS AND METHODS

2.1 | Guacamole

The guacamole was prepared from ripe avocados (375 g), tomatoes (100 g), white onions (75 g), cilantro (3 g), NaCl (4 g), pepper sauce (Tabasco[®], 2 g), and Tahiti lime juice (50 g). All components were homogenized in an industrial blender (BM2 Maxi blender; Skymesen) for 5 min, then stored at -25°C until film preparation. Its solid content, as determined by gravimetry after drying at 105°C in a drying oven until constant weight, was 19%.

2.2 | Preparation of films

Ten films were prepared according to a simplex centroid mixture design (previously used and explained by Freitas et al., 2022), according to Table 1, with three components, namely: guacamole, matrix (sodium alginate TICA-algin 400 F, lot 41369; Tic Gums), and glycerol, in proportion ranges defined from preliminary tests. All the film-forming dispersions were prepared in volumes around 400 mL, and the amounts of distilled water were calculated to assure that all dispersions had the same solid content (35%). Alginate and glycerol were dispersed in water and homogenized in an Ultra-Turrax T18 (IKA) at 24,000 rpm for 15 min. The guacamole was then added to the dispersion, which was homogenized again in the Ultra-Turrax for 10 min. This step was done in a beaker immersed in an ice bath (to avoid heating the dispersion, which had caused the guacamole to become bitter in preliminary tests). Each dispersion was then vacuum degassed, cast onto polyester (Mylar[®])-lined 400×300 mm glass plates to a thickness of

TABLE 1 Film formulations (component % proportions followed by pseudocomponents in parentheses).

Film	Proportions		
	Guacamole (dry basis)	Alginate	Glycerol
1	40 (1)	45 (0)	15 (0)
2	25 (0)	60 (1)	15 (0)
3	25 (0)	45 (0)	30 (1)
4	32.5 (0.5)	52.5 (0.5)	15 (0)
5	32.5 (0.5)	45 (0)	22.5 (0.5)
6	25 (0)	52.5 (0.5)	22.5 (0.5)
7	30 (0.33)	50 (0.33)	20 (0.33)
8	35 (0.67)	47.5 (0.17)	17.5 (0.17)
9	27.5 (0.17)	55 (0.67)	17.5 (0.17)
10	27.5 (0.17)	47.5 (0.17)	25 (0.67)

2 mm, and oven-dried in an air-circulating oven (SL102; Solab) at 30°C for 16 h.

Crosslinking tests have been carried out by immersing the cast films into CaCl_2 solutions at different concentrations (0.5% and 1%) for 1 min before the drying step, but the crosslinked films presented a wrinkled appearance and extreme brittleness after drying, and that is why the films were produced without a crosslinking step.

The films were then detached from the substrates and cut into test samples (according to the dimensions required for each test), whose thicknesses were measured with an Akrom KR1250 coating thickness tester (Akrom) to the nearest $1 \mu\text{m}$. The test samples were then conditioned for at least 40 h at 25°C and 50% RH in an Ethik 420-2TS climatic chamber (Nova Ética) before the analyses.

2.3 | Film characterization

The solid contents of the films have been determined by gravimetry after drying at 105°C in a drying oven until constant weight.

The scanning electron microscopy was carried out in a JSM-6510 microscope (Jeol) for the film that presented the best overall properties (especially the lowest WVP) and also for a control alginate film with 30% glycerol (for comparing images and structures). Film samples were mounted on aluminium stubs using conductive carbon tape and sputter-coated with gold for 60 s at 40 mA with an SCD 050 Sputter Coater (BAL-TEC), with their film-air surfaces (as the films were dried) facing upward. Other specimens were immersed in liquid nitrogen for 5 min, fractured with tweezers, and mounted on aluminium stubs with the fractured surface facing upward, using conductive carbon tape, then sputter-coated with

gold. The samples were examined using an accelerating voltage of 5 kV at $\times 1500$ magnification for surfaces and $\times 1000$ for cross-sections.

The Fourier-transform infrared (FTIR) spectra of the films were recorded by using a Vertex 70 FTIR spectrometer (Bruker) in Attenuated Total Reflectance mode (ATR) equipped with a diamond crystal accessory, in the $4000\text{--}500\text{ cm}^{-1}$ range, with a 4-cm^{-1} resolution over 32 scans.

The water vapor permeability (WVP) determination was based on an ASTM method (E96/E96M-16, (ASTM, 2016), with eight replicates. Polytetrafluoroethylene (PTFE) permeation cells (24 mm in diameter, 10 mm in height), each containing 1.5 mL of distilled water, were placed in an Ethik 420-2TS climatic chamber at 25°C and 50% RH. Eight weight measurements were taken within 24–36 h. The WVP values have been calculated according to the equation:

$$\text{WVP} = \Delta w \times L / (\Delta t \times A \times (p_1 - p_2)). \quad (1)$$

$\Delta w/\Delta t$ being the weight loss per time; L , the film thickness; A , the exposed area of the film; and p_1 and p_2 , the partial vapor pressures of water vapor on the inside and outside of the test film, respectively, given as $p_1 = P_{\text{sat}} \times \text{RH}_{\text{in}}$ and $p_2 = P_{\text{sat}} \times \text{RH}_{\text{out}}$. RH_{in} and RH_{out} are the relative humidities of the internal and external sides (100% and test RH respectively) of the film, and P_{sat} is the saturated vapor pressure at the test temperature (25°C).

The water contact angles (WCA) were determined (in quadruplicate) with a KSV CAM 101 Optical Contact Angle Meter (KSV Instruments) equipped with a CCD KSV-5000 camera. Each measurement was taken from a $4\text{-}\mu\text{L}$ drop of Milli-Q water on the film surface, and images were registered from 0 to 3 s.

The tensile strength and elongation of $125 \times 12.5\text{ mm}$ films specimens were measured (with 12 replicates) according to the method D882-12 (ASTM, 2012), with an Emic DL-3000 Universal Testing Machine (load cell of 100 N, initial grip separation of 100 mm, and cross-head speed of 12.5 mm min^{-1}).

The formulation exhibiting the lowest WVP was tested for its ability to reduce the texture changes in nachos exposed to tomato sauce. Triangular nachos with about 50 mm in side (Doritos[®]; Pepsico) were divided into three treatments (with seven nachos per treatment), according to Figure 1. In one treatment (NT), each nacho was covered with 2 g tomato sauce (Pomarola, Cargill, with 14.2 wt% solids, including 10.8 wt% carbohydrates, 1.7 wt% proteins, and 1.5 wt% dietary fiber). In another (NFT), a film sample (covering the entire nacho surface) was placed between the nacho and the tomato sauce (2 g). Finally, a control treatment (N) consisted of nachos without film or sauce. All nachos were left on a lab bench at 25°C for 50 min, then the films and/or tomato sauce were removed from their surfaces, and the

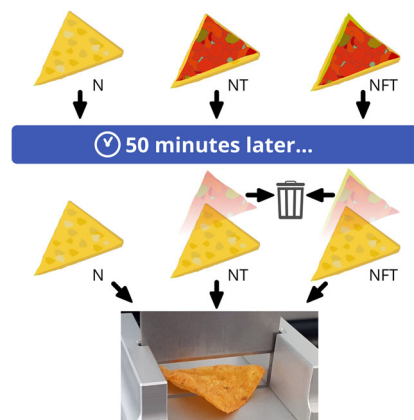


FIGURE 1 Test for texture changes of nachos: N, control nachos, without film or tomato sauce; NFT, nachos covered with film and tomato sauce; NT, nachos covered with tomato sauce.

nachos were subjected to a texture analysis on a TA.XT Plus texture analyzer (Stable Micro Systems) equipped with a TA-42 knife probe with a 45-degree chisel blade cutting through the nachos at a crosshead speed of 2 mm s^{-1} and posttest speed of 10 mm s^{-1} . The fracture force and the area under the force-distance curve were recorded, representing hardness and toughness respectively, by using the software Exponent (Stable Micro Systems).

2.4 | Data processing and statistical analyses

The results were analyzed using Minitab[®] statistical software v. 19 (Minitab Inc). The model adjustment was made in terms of pseudo-components. Moreover, the differences between treatments were analyzed by one-way ANOVA followed by Tukey's post hoc tests, with a confidence level of 95%.

3 | RESULTS AND DISCUSSION

All the films presented a uniform yellowish appearance, with about 93% solids.

The experimental responses to all treatments as well as the regression coefficients for the statistic models (in pseudocomponents) are presented at Table 2. All the models were significant ($p < 0.05$), although the one for WCA was only significant when the interaction terms were removed, creating a linear model. Except for the WCA model, all of them presented coefficients of determination (R^2 values) higher than 70%.

Figure 2 presents the contour plots for the models. Alginate was the component with the highest effect on the tensile strength (Table 2, Figure 2), which explains why the film #2 (the one with most alginate) was the strongest one (Table 2), while higher glycerol and

TABLE 2 Experimental responses and regression coefficients for the corresponding models.

Films	Gua/alg/gly ^a ratios	Responses			
		σ (MPa)	ϵ (%)	WVP (g mm kPa ⁻¹ h ⁻¹ m ⁻²)	WCA (°)
1	40/45/15	15.73 ^c	17.16 ^{bcd}	4.589 ^{ab}	86.17 ^a
2	25/60/15	28.88 ^a	10.09 ^d	3.605 ^c	74.33 ^b
3	25/45/30	10.66 ^d	31.14 ^a	5.187 ^a	61.39 ^c
4	32.5/52.5/15	21.93 ^b	10.49 ^d	3.862 ^{bc}	81.49 ^a
5	32.5/45/22.5	11.81 ^{cd}	21.55 ^b	4.553 ^{ab}	82.46 ^a
6	25/52.5/22.5	20.67 ^b	18.85 ^{bc}	3.934 ^{bc}	66.01 ^c
7	30/50/20	21.04 ^b	19.48 ^b	4.397 ^{abc}	80.46 ^{ab}
8	35/47.5/17.5	13.97 ^{cd}	12.97 ^{cd}	4.626 ^{ab}	83.15 ^a
9	27.5/55/17.5	21.06 ^b	10.66 ^d	3.876 ^{bc}	64.45 ^c
10	27.5/47.5/25	13.89 ^{cd}	22.47 ^b	4.769 ^a	62.93 ^c

Terms	Coefficients			
	σ	ϵ	WVP	WCA
β_1	15.22	16.52	4.60	90.30
β_2	28.30	9.71	3.56	70.68
β_3	10.70	31.06	5.18	61.87
β_{12}	-1.70	-11.90	-0.15	-
β_{13}	-4.50	-9.12	-0.47	-
β_{23}	4.50	-5.29	-1.10	-
R^2 (% , adjusted)	83.76	88.76	81.07	68.96
F Value	10.29	15.22	8.71	11.00
p Value	0.02	0.01	0.03	<0.01

Note: Values in the same column sharing at least one common letter (or not followed by letters) are not significantly different ($p > 0.05$). β_1 , β_2 , β_3 , β_{12} , β_{13} , β_{23} : Terms for guacamole, alginate, glycerol, and respective interactions (as pseudo-components).

Abbreviations: WCA, water contact angle at 2 s; WVP, water vapor permeability; ϵ , elongation at break (%); σ , tensile strength.

^aGuacamole/alginate/glycerol weight ratios (on a dry basis).

guacamole contents decreased the tensile strength, due to the plasticizing effects of glycerol and the guacamole lipids (Dong et al., 2023; Miller et al., 2021). The elongation, on the other hand, was mostly increased by glycerol (and also by guacamole, to a lower extent) and decreased by alginate, which corroborates several studies reporting the effects of glycerol (Dong et al., 2023; Hazrati et al., 2021; Zhang et al., 2016) and lipids (Miller et al., 2021) as plasticizers, enhancing elongation but decreasing tensile strength of films.

The WVP was mostly decreased by the alginate content, whereas glycerol was the component that mostly increased it (Table 2, Figure 2), which is also related with the plasticizer effect of glycerol, decreasing molecular bonding and increasing the solubility coefficient to water vapor (Miller et al., 2021). The treatment #2 (with the highest alginate content), being the one with the lowest WVP, was considered as the best film for the intended application (i.e., as a moisture barrier in multicomponent

foods), besides having presented the highest tensile strength (Table 2). Although the model for WCA was not significant, the films with the highest guacamole contents were the ones with highest WCA (Table 2), indicating that the presence of high guacamole contents enhanced their hydrophobicity, since avocado has a lipid content that corresponds to more than half its dry weight (Dreher & Davenport, 2013), while glycerol was the component that mostly decreased WCA, due to its high polarity. However, the highest hydrophobicity values provided by guacamole did not reflect in the lowest WVP values, probably because the presence of a hydrophobic phase on the hydrophilic matrix promoted the formation of discontinuities, thus increasing water diffusivity, that is to say, the lipids acted as plasticizers (Yousuf et al., 2022), increasing the polymer chain spaces, thus increasing water vapor diffusivity. The effect of lipids on increasing WVP corroborates findings from previous studies (Chen et al., 2022; Medeiros et al., 2022), whereas

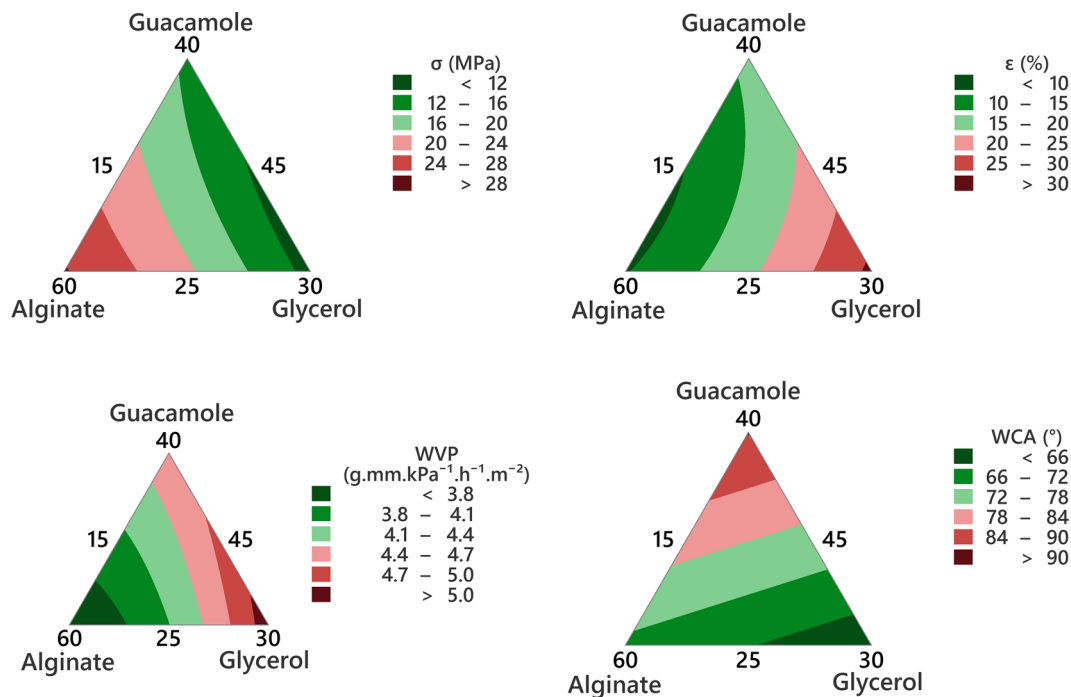


FIGURE 2 Contour plots for the film properties.

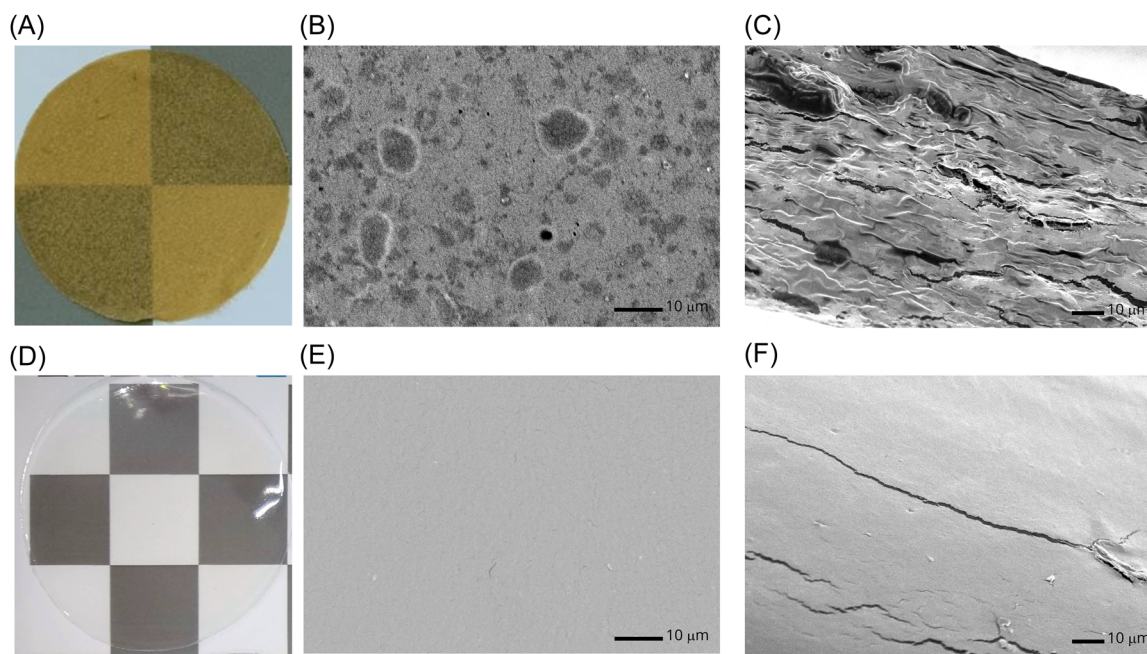


FIGURE 3 Top: Film #2 (with 25% guacamole, 50% alginate, and 15% glycerol, d.b.), A, B, and C representing a photograph, and scanning electron microscopy (SEM) images of a plain surface and cross-section, respectively. Down: control alginate film with 30% glycerol, D, E, and F representing a photograph, and SEM images of a plain surface and cross-section, respectively.

other studies have reported that the presence of lipids have exhibited the opposite effect, that is to say, they lowered the WVP, due to their effect on hydrophobicity (Oliveira Filho et al., 2020; Sothornvit, 2010).

The micrographs of the film #2 (the one with the best overall properties) and a control alginate film were

presented along with the corresponding photographs (Figure 3). While the alginate film was quite transparent and with a smooth surface (although with some cracks on the cross-section), film #2 was yellowish and translucent, with a rough surface, and presenting pores/discontinuities revealing the existence of hydrophobic areas, which are

due to the high lipid content of avocado mesocarp (Tan, 2019). Those discontinuities corroborate the previously mentioned increased water diffusivity resulting from high guacamole contents. The films obtained by Freitas et al. (2022), also containing a hydrophobic phase, presented pores and discontinuities as well.

In the FTIR spectra (Figure 4), the broad band around 3300 cm^{-1} (present in both the film and its components) is linked to OH stretching vibrations of OH groups (Lozano-Vazquez et al., 2021). The band at 1592 cm^{-1} in alginate is ascribed to asymmetric stretching of —COO^- (Aydin & Zorlu, 2022; Wang et al., 2016), and was shifted to a higher wavenumber in the film, due to the interference of the C=C stretching band of aromatic rings of phenolic groups in guacamole around 1600 cm^{-1} (Dhaouadi et al., 2021). The band from symmetric stretching of —COO^- at 1405 cm^{-1} (Wang et al., 2016) also presented a shift in the film, which is due to the interference by the CH_2 bending of lipids in guacamole at around 1420 cm^{-1} (Qiu et al., 2020). Other bands from alginate include those from C—O—C stretching between 1130 and 1020 cm^{-1} (Abou-Zeid et al., 2019; Vaziri et al., 2018), the one from O—H deformation at 944 cm^{-1} (Pereira et al., 2003), and the one from mannuronic acid residues at 810 cm^{-1} (Costa et al., 2018). Bands mainly due to the presence of avocado (in guacamole) include those from CH_3 stretching and CH_2 symmetric stretching at 2923 and 2846 cm^{-1} respectively (Contreras-Ramírez et al., 2021), the one from C=O stretching vibrations of aldehydes, ketones and carboxylic acids at 1745 cm^{-1} (Manaf et al., 2018), those between 1238 and around 1030 cm^{-1} , ascribed to

C—O stretching (Manaf et al., 2018), and the one at 902 cm^{-1} from $=\text{CH}_2$ wagging (Rohman et al., 2016).

The loss of crispiness in nachos previously covered (for 50 min) with either tomato sauce (NT) or a film sample and tomato sauce (NFT) are presented in Figure 5, when compared to uncovered nachos (N). For the three measured attributes, the pure nachos presented the lowest values, as

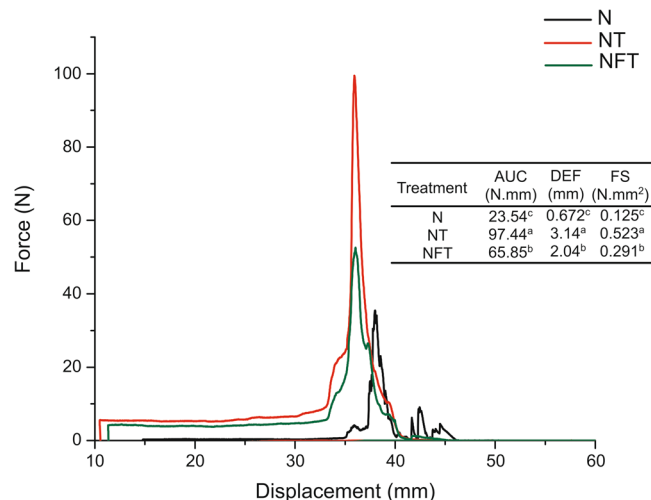


FIGURE 5 Instrumental texture of nachos: uncovered (N); previously covered for 50 min with tomato sauce (NT) or a film sample and tomato sauce (NFT). AUC, area under the curve for the major fracture event, representing the energy taken for the nacho to be fractured; DEF, deformation of the nacho on the major fracture event; FS, fracture strength (maximum force at the major fracture event divided by the area of the nacho in contact with the probe).

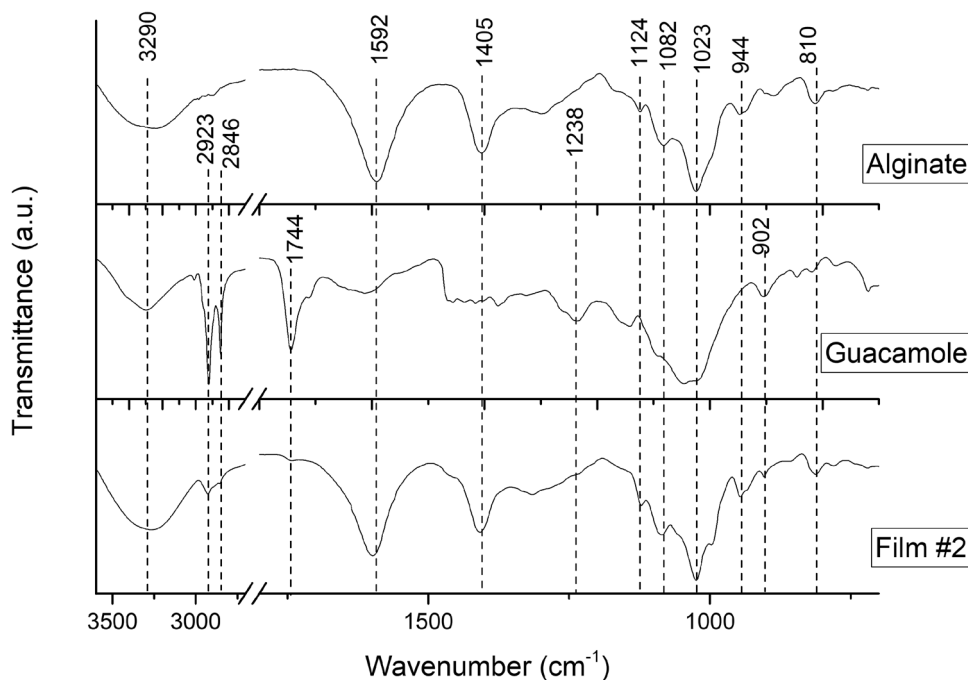


FIGURE 4 Fourier-transform infrared spectra of film #2 and its main components (powder alginate and freeze-dried guacamole).

expected, indicating that the nachos not previously covered with a moist tomato sauce were easier to fracture (requiring less energy to fracture and deforming less). The previously covered nachos required higher forces and energy to be fractured, and were more deformed, indicating loss of crispiness. However, when compared to the nachos previously covered only with the tomato sauce (NT), the ones in which a film sample was inserted between the nachos and the tomato sauce (NFT) presented lower values for the three attributes, that is, they were crispier. Thus, it was demonstrated that the presence of an alginate-based film containing guacamole was able to reduce the crispiness loss of nachos on a short storage. Similarly, the results by Freitas et al. (2022) also demonstrated that the presence of a polysaccharide-based film between nachos and a moist sauce contributed to maintain the crispiness of the nachos.

4 | CONCLUSIONS

Edible films containing different proportions of alginate, guacamole, and glycerol were successfully formed, according to a simplex centroid mixture design. While alginate was the most contributing component to increase the film strength and to reduce its WVP, the presence of guacamole favored the film hydrophobicity. Both guacamole (due to its lipid contents) and glycerol acted as plasticizers, decreasing the tensile strength and increasing film elongation, while also increasing WVP. The film with the lowest WVP, when inserted between nachos and tomato sauce, was able to reduce the crispiness loss of nachos during a short (50-min) storage, and could be thus useful on the context of delivery of multicomponent foods (e.g., tacos) for which the loss of crispiness is an issue.

AUTHOR CONTRIBUTIONS

Matheus Carvalho Matos: Investigation. **Jackson Andson de Medeiros:** Investigation; writing—review & editing. **Leticia Bueno Santos:** Investigation; methodology. **Henriette M. C. de Azeredo:** Conceptualization; formal analysis; methodology; project administration; resources; validation; writing—original draft.

ACKNOWLEDGMENTS

Authors Matos, Medeiros, and Santos acknowledge the National Council for Scientific and Technological Development (CNPq) and the Coordination for the Improvement of Higher Education Personnel (CAPES) for their scholarships (CNPq 134100/2019-0, CNPq 161930/2021-2, and CAPES 88887.706251/2022-00 respectively). Author Azeredo thanks CNPq for her Research Productivity Fellowship (308777/2021-2). The authors also thank Ingredient Brazil for providing us with the sodium alginate used in this study.

CONFLICT OF INTEREST STATEMENT

The authors declare no conflicts of interest.

ETHICS STATEMENT

None declared.

ORCID

Henriette M. C. de Azeredo  <https://orcid.org/0000-0002-9295-4682>

REFERENCES

- Abou-Zeid, R. E., Awad, N. S., Nabil, S., Salama, A., & Youssef, M. A. (2019). Oxidized alginate/gelatin decorated silver nanoparticles as new nanocomposite for dye adsorption. *International Journal of Biological Macromolecules*, *141*, 1280–1286. <https://doi.org/10.1016/j.ijbiomac.2019.09.076>
- ASTM. (2012). Standard test method for tensile properties of thin plastic sheeting (ASTM D882-12), *Annual book of American standard testing methods*. American Society for Testing and Materials.
- ASTM. (2016). Standard test method for water vapor transmission of materials (E96/E96M-16), *Annual book of American standard testing methods*. American Society for Testing and Materials.
- Aydin, G., & Zorlu, E. B. (2022). Characterisation and antibacterial properties of novel biodegradable films based on alginate and roselle (*Hibiscus sabdariffa* L.) extract. *Waste and Biomass Valorization*, *13*, 2991–3002. <https://doi.org/10.1007/s12649-022-01710-3>
- Azeredo, H. M. C., Morrugares-Carmona, R., Wellner, N., Cross, K., Bajka, B., & Waldron, K. W. (2016). Development of pectin films with pomegranate juice and citric acid. *Food Chemistry*, *198*, 101–106. <https://doi.org/10.1016/j.foodchem.2015.10.117>
- Azeredo, H. M. C., Otoni, C. G., & Mattoso, L. H. C. (2022). Edible films and coatings—Not just packaging materials. *Current Research in Food Science*, *5*, 1590–1595. <https://doi.org/10.1016/j.crfs.2022.09.008>
- Chen, H., Wu, C., Feng, X., He, M., Zhu, X., Li, Y., & Teng, F. (2022). Effects of two fatty acids on soy protein isolate/sodium alginate edible films: Structures and properties. *LWT*, *159*, 113221. <https://doi.org/10.1016/j.lwt.2022.113221>
- Contreras-Ramirez, J. I., Villanueva-Fierro, I., González-Laredo, R. F., Toro-Vázquez, J. F., Pérez-Martínez, J. D., Rosas-Flores, W., & Gallegos-Infante, J. A. (2021). Study of the relationship of hydrogen bonding and hydrophobic interactions in W/O organogel emulsions by Raman microspectroscopy. *Colloid and Interface Science Communications*, *44*, 100486. <https://doi.org/10.1016/j.colcom.2021.100486>
- Costa, M. J., Marques, A. M., Pastrana, L. M., Teixeira, J. A., Sillankorva, S. M., & Cerqueira, M. A. (2018). Physicochemical properties of alginate-based films: Effect of ionic crosslinking and mannuronic and guluronic acid ratio. *Food Hydrocolloids*, *81*, 442–448. <https://doi.org/10.1016/j.foodhyd.2018.03.014>
- Dhaouadi, F., Sellaoui, L., Hernández-Hernández, L. E., Bonilla-Petriciolet, A., Mendoza-Castillo, D. I., Reynel-Ávila, H. E., González-Ponce, H. A., Taamalli, S., Louis, F., & Lamine, A. B. (2021). Preparation of an avocado seed hydrochar and its application as heavy metal adsorbent: Properties and advanced statistical physics modeling. *Chemical Engineering Journal*, *419*, 129472. <https://doi.org/10.1016/j.cej.2021.129472>
- Dong, Y., Li, Y., Ma, Z., Rao, Z., Zheng, X., Tang, K., & Liu, J. (2023). Effect of polyol plasticizers on properties and microstructure of soluble soybean polysaccharide edible films. *Food Packaging and Shelf Life*, *35*, 101023. <https://doi.org/10.1016/j.foodpl.2022.101023>
- Dreher, M. L., & Davenport, A. J. (2013). Hass avocado composition and potential health effects. *Critical Reviews in Food Science and Nutrition*, *53*, 738–750. <https://doi.org/10.1080/10408398.2011.556759>
- Freitas, J., Mendonça, G., Santos, L., Alonso, J., Mendes, J., Barud, H., & Azeredo, H. (2022). Bacterial cellulose/tomato puree edible films as moisture barrier structures in multicomponent foods. *Foods*, *11*, 2336. <https://doi.org/10.3390/foods11152336>
- Hazrati, K. Z., Sapuan, S. M., Zuhri, M. Y. M., & Jumaidin, R. (2021). Effect of plasticizers on physical, thermal, and tensile

- properties of thermoplastic films based on *Dioscorea hispida* starch. *International Journal of Biological Macromolecules*, *185*, 219–228. <https://doi.org/10.1016/j.ijbiomac.2021.06.099>
- Kadzińska, J., Bryś, J., Ostrowska-Ligęza, E., Estéve, M., & Janowicz, M. (2020). Influence of vegetable oils addition on the selected physical properties of apple–sodium alginate edible films. *Polymer Bulletin*, *77*, 883–900. <https://doi.org/10.1007/s00289-019-02777-0>
- Kelso, A. (2019). *Maintaining mouthfeel: The challenge of preserving food texture on the shelf and during delivery*. <https://www.fooddive.com/news/maintaining-mouthfeel-the-challenge-of-preserving-food-texture-on-the-shelf/557085/>
- Lozano-Vazquez, G., Alvarez-Ramirez, J., Lobato-Calleros, C., Vernon-Carter, E. J., & Hernández-Marin, N. Y. (2021). Characterization of corn starch-calcium alginate xerogels by microscopy, thermal, XRD, and FTIR analyses. *Starch - Stärke*, *73*, 2000282. <https://doi.org/10.1002/star.202000282>
- Manaf, Y. N., Rahardjo, A. P., Yusof, Y. A., Desa, M. N., & Nusantoro, B. P. (2018). Lipid characteristics and tocopherol content of the oils of native avocado cultivars grown in Indonesia. *International Journal of Food Properties*, *21*, 2758–2771. <https://doi.org/10.1080/10942912.2018.1564761>
- Medeiros, J. A., Otoni, C. G., Niro, C. M., Sivieri, K., Barud, H. S., Guimarães, F. E. G., Alonso, J. D., & Azeredo, H. M. C. (2022). Alginate films as carriers of probiotic bacteria and pickering emulsion. *Food Packaging and Shelf Life*, *34*, 100987. <https://doi.org/10.1016/j.foodpack.2022.100987>
- Melo, P. T. S., Nunes, J. C., Otoni, C. G., Aouada, F. A., & Moura, M. R. (2019). Combining cupuassu (*Theobroma grandiflorum*) puree, pectin, and chitosan nanoparticles into novel edible films for food packaging applications. *Journal of Food Science*, *84*(8), 2228–2233. <https://doi.org/10.1111/1750-3841.14685>
- Miller, K., Silcher, C., Lindner, M., & Schmid, M. (2021). Effects of glycerol and sorbitol on optical, mechanical, and gas barrier properties of potato peel-based films. *Packaging Technology and Science*, *34*, 11–23. <https://doi.org/10.1002/pts.2536>
- Munhoz, D. R., Moreira, F. K. V., Bresolin, J. D., Bernardo, M. P., De Sousa, C. P., & Mattoso, L. H. C. (2018). Sustainable production and in vitro biodegradability of edible films from yellow passion fruit coproducts via continuous casting. *ACS Sustainable Chemistry & Engineering*, *6*, 9883–9892. <https://doi.org/10.1021/acssuschemeng.8b01101>
- O'Connor, L. J., Favreau-Farhadi, N., & Barrett, A. H. (2018). Use of edible barriers in intermediate moisture food systems to inhibit moisture migration. *Journal of Food Processing and Preservation*, *42*, e13512. <https://doi.org/10.1111/jfpp.13512>
- Oliveira, E. F. R., Bonfim, K. S., Aouada, F. A., Azeredo, H. M. C., & Moura, M. R. (2023). A sustainable approach on the potential use of kale puree in edible wraps. *Applied Food Research*, *3*, 100261. <https://doi.org/10.1016/j.afres.2022.100261>
- Oliveira, W. Q., Azeredo, H., Neri-Numa, I. A., & Pastore, G. M. (2021). Food packaging wastes amid the COVID-19 pandemic: Trends and challenges. *Trends in Food Science & Technology*, *116*, 1195–1199. <https://doi.org/10.1016/j.tifs.2021.05.027>
- Oliveira Filho, J. G., Bezerra, C. C. O. N., Albiero, B. R., Oldoni, F. C. A., Miranda, M., Egea, M. B., Azeredo, H. M. C., & Ferreira, M. D. (2020). New approach in the development of edible films: The use of carnauba wax micro- or nanoemulsions in arrowroot starch-based films. *Food Packaging and Shelf Life*, *26*, 100589. <https://doi.org/10.1016/j.foodpack.2020.100589>
- Otoni, C. G., Avena-Bustillos, R. J., Azeredo, H. M. C., Lorevice, M. V., Moura, M. R., Mattoso, L. H. C., & McHugh, T. H. (2017). Recent advances on edible films based on fruits and vegetables—A review. *Comprehensive Reviews in Food Science and Food Safety*, *16*, 1151–1169. <https://doi.org/10.1111/1541-4337.12281>
- Pereira, L., Sousa, A., Coelho, H., Amado, A. M., & Ribeiro-Claro, P. J. A. (2003). Use of FTIR, FT-Raman and ¹³C-NMR spectroscopy for identification of some seaweed phycocolloids. *Biomolecular Engineering*, *20*, 223–228. [https://doi.org/10.1016/S1389-0344\(03\)00058-3](https://doi.org/10.1016/S1389-0344(03)00058-3)
- Qiu, S., Weng, Y., Li, Y., Chen, Y., Pan, Y., Liu, J., Lin, W., Chen, X., Li, M., Lin, T., Liu, W., Zhang, L., & Lin, D. (2020). Raman profile alterations of irradiated human nasopharyngeal cancer cells detected with laser tweezer Raman spectroscopy. *RSC Advances*, *10*, 14368–14373. <https://doi.org/10.1039/D0RA01173H>
- Rangel-Marrón, M., Mani-López, E., Palou, E., & López-Malo, A. (2019). Effects of alginate-glycerol-citric acid concentrations on selected physical, mechanical, and barrier properties of papaya puree-based edible films and coatings, as evaluated by response surface methodology. *LWT*, *101*, 83–91. <https://doi.org/10.1016/j.lwt.2018.11.005>
- Rohman, A., Windarsih, A., Riyanto, S., Sudjadi, Shuhel Ahmad, S. A., Rosman, A. S., & Yusoff, F. M. (2016). Fourier transform infrared spectroscopy combined with multivariate calibrations for the authentication of avocado oil. *International Journal of Food Properties*, *19*, 680–687. <https://doi.org/10.1080/10942912.2015.1039029>
- Sothornvit, R. (2010). Physical and mechanical properties of composite mango films. *Acta horticulturae*, *877*, 973–978. <https://doi.org/10.17660/ActaHortic.2010.877.131>
- Tan, C. X. (2019). Virgin avocado oil: An emerging source of functional fruit oil. *Journal of Functional Foods*, *54*, 381–392. <https://doi.org/10.1016/j.jff.2018.12.031>
- Vaziri, A. S., Alemzadeh, I., & Vossoughi, M. (2018). Improving survivability of *Lactobacillus plantarum* in alginate-chitosan beads reinforced by Na-tripolyphosphate dual cross-linking. *LWT*, *97*, 440–447. <https://doi.org/10.1016/j.lwt.2018.07.037>
- Viana, R. M., Sá, N. M. S. M., Barros, M. O., Borges, M. F., & Azeredo, H. M. C. (2018). Nanofibrillated bacterial cellulose and pectin edible films added with fruit purees. *Carbohydrate Polymers*, *196*, 27–32. <https://doi.org/10.1016/j.carbpol.2018.05.017>
- Wang, F., Lu, X., & Li, X. (2016). Selective removals of heavy metals (Pb²⁺, Cu²⁺, and Cd²⁺) from wastewater by gelation with alginate for effective metal recovery. *Journal of Hazardous Materials*, *308*, 75–83. <https://doi.org/10.1016/j.jhazmat.2016.01.021>
- Yousuf, B., Sun, Y., & Wu, S. (2022). Lipid and lipid-containing composite edible coatings and films. *Food Reviews International*, *38*, 574–597. <https://doi.org/10.1080/87559129.2021.1876084>
- Zhang, P., Zhao, Y., & Shi, Q. (2016). Characterization of a novel edible film based on gum ghatti: Effect of plasticizer type and concentration. *Carbohydrate Polymers*, *153*, 345–355. <https://doi.org/10.1016/j.carbpol.2016.07.082>

How to cite this article: de Matos, M. C., de Medeiros, J. A., Santos, L. B., & de Azeredo, H. M. C. (2023). Alginate/guacamole edible films as moisture barrier layers in multicomponent foods. *eFood*, *4*(4), e109. <https://doi.org/10.1002/efd2.109>